Interface Structures of Gold Nanoparticles on TiO2 (110)

AUTHOR(S):

Shibata, N.; Goto, A.; Matsunaga, K.; Mizoguchi, T.; Findlay, S. D.; Yamamoto, T.; Ikuhara, Y.

CITATION:

Shibata, N. ...[et al]. Interface Structures of Gold Nanoparticles on TiO2 (110). Physical Review Letters 2009, 102(13): 136105.

ISSUE DATE:

2009-04

URL:

http://hdl.handle.net/2433/109848

Interface Structures of Gold Nanoparticles on TiO_2 (110)

N. Shibata,[1,2,*] A. Goto,[1] K. Matsunaga,[3,4] T. Mizoguchi,[1] S. D. Findlay,[1] T. Yamamoto,[1,4] and Y. Ikuhara[1,4,5]

[1]*Institute of Engineering Innovation, School of Engineering, The University of Tokyo, Bunkyo-ku, Tokyo 113-8656, Japan*
[2]*PRESTO, Japan Science and Technology Agency, 4-1-8 Honcho Kawaguchi, Saitama 332-0012, Japan*
[3]*Department of Materials Science and Engineering, Kyoto University, Yoshida- Honmachi, Sakyo, Kyoto 606-8501, Japan*
[4]*Nanostructures Research Laboratory, Japan Fine Ceramic Center, 2-4-1 Mutsuno, Atsuta-ku, Nagoya 456-8587, Japan*
[5]*WPI Advanced Institute for Materials Research, Tohoku University, 2-1-1, Katahira, Aoba-ku, Sendai 980-8577, Japan*

(Received 16 September 2008; published 3 April 2009)

Scanning transmission electron microscopy and density functional theory are used to characterize atomic structures of nanoscale heterointerfaces between gold nanoparticles and a TiO_2 (110) surface. It is found that when the gold nanoparticle size is smaller than a few nanometers, gold atoms preferentially attach to specific sites on the TiO_2 surface and thus form an epitaxial and coherent heterointerface. Conversely, as the gold size becomes larger, the gold-TiO_2 interface loses lattice coherency in order to accommodate the large lattice mismatch between the two dissimilar crystals.

DOI: 10.1103/PhysRevLett.102.136105 PACS numbers: 68.35.−p, 61.46.Df, 68.37.Ma

Gold nanoparticles dispersed on metal-oxide supports are active catalysts for a variety of chemical reactions [1–4]. It has been demonstrated that the unique catalytic activity strongly depends on the size of Au nanoparticles and the type of metal-oxide support [2,5], suggesting the importance of Au-support interfacial interactions on a nanometer scale. However, a detailed description of nanoscale heterointerface formation has not been established, especially its relation to the Au nanoparticle size, and the size-dependent catalytic activity of supported Au is still a matter of conjecture. It is thus essential to characterize the atomic structure of nanosized Au-support interfaces in order to truly understand the origin of the remarkable catalytic activity with strong particle size dependency.

Atomic-resolution scanning transmission electron microscopy (STEM) is a powerful method for characterizing metal cluster catalysts at subnanometer dimensions [6,7]. Under the high-angle annular dark-field (HAADF) imaging mode, the STEM image can be considered as an incoherent image, and the image intensity strongly depends on the atomic number (Z) of the constituent atoms [8]. In this study, Au/TiO_2 (110) model catalysts were fabricated and atomic-resolution plan-view STEM imaging was carried out to directly observe the atomic structures of Au nanoparticles on the TiO_2 (110) surface. The observed structures are interpreted using first-principles density functional theory (DFT) calculations.

A commercially available rutile TiO_2 (110) substrate was thinned down by mechanical polishing followed by ion bombardment to obtain electron transparent TEM samples. The TEM samples were annealed in air at 973 K for 30 min to produce atomically flat (110) surfaces, in accordance with previous reports [9–11]. High-purity gold (99.95%) was deposited on the TEM sample surface by vacuum evaporation at room temperature with a base pressure of about 1×10^{-3} Pa. Atomic-resolution HAADF STEM images were taken with a 200-kV JEM-2100F TEM-STEM electron microscope (JEOL Ltd., Tokyo, Japan) equipped with an aberration corrector (CEOS GmbH, Heidelberg, Germany). A HAADF detector with an inner angle greater than 70 mrad was used for the STEM observations.

Figure 1(a) shows a HAADF STEM image of a rutile TiO_2 crystal observed in the ⟨110⟩ projection. There are two types of bright spots with different image intensities as indicated by the arrows. These bright spots correspond to the two different Ti-containing columns as shown schematically in Fig. 1(b). The brighter spots correspond to the atomic columns with both Ti and O atoms (Ti-O columns),

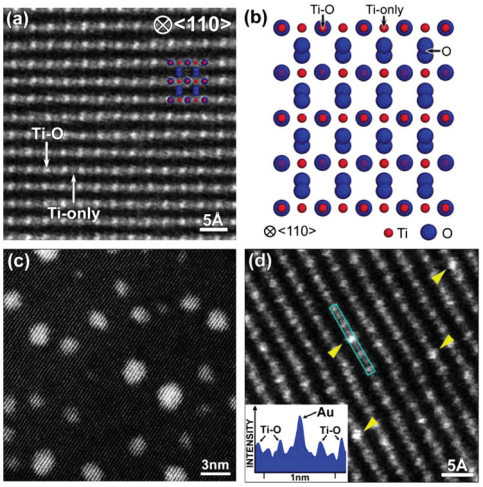

FIG. 1 (color). (a) Atomic-resolution HAADF STEM image of a rutile TiO_2 single crystal observed from ⟨110⟩ direction. (b) The corresponding crystal structure model. (c) Typical HAADF STEM image of Au nanoparticles deposited on a TiO_2 (110) surface. (d) HAADF STEM image of single Au atoms on the TiO_2 (110) surface. Inset shows the image intensity profile across a single Au atom, showing strong image intensity on the Ti-O columns.

while the darker spots correspond to the atomic columns with body-centered Ti atoms only (Ti-only columns), as confirmed by HAADF STEM simulation [12]. The signal from the oxygen columns is extremely weak, and thus the troughs in between the Ti-containing columns appear dark. Figure 1(c) shows a typical HAADF STEM image of Au nanoparticles deposited on the TiO_2 (110) surface. The Au nanoparticles on the TiO_2 surface are clearly visible due to the strong Z-dependent image contrast (Z: Au = 79, Ti = 22, O = 8). The projected Au nanoparticle sizes are in the range 1–5 nm. Figure 1(d) shows single Au atoms attached on the TiO_2 (110) surface as indicated by the arrows. The strong image intensity of the Au single atoms is preferentially found on top of Ti-O columns. This site corresponds to the on-top sites of bridging O sites (O_{br}) or fivefold Ti sites on the stoichiometric TiO_2 (110) surface.

Previous scanning tunnel microscopy studies and DFT calculations showed that Au atom adsorption on the TiO_2 (110) surface strongly depends on the surface chemistry [13–18]. If the surface is stoichiometric, Au adsorption on top of the fivefold coordinated Ti sites is most energetically stable [13,14,17]. If the surface is reduced and O_{br} vacancies are introduced, Au atoms are most stable on the O_{br} vacancy sites [13–16,18]. These two possibilities agree well with our STEM images. On the other hand, if the surface is oxidized or hydrated, the stable attachment sites become inconsistent with our images [14,18]. The observed Au single atoms are thus considered to be either on the fivefold coordinated Ti sites or the O_{br} vacancy sites on the TiO_2 (110) surface. In the present experiment, however, there should be a certain amount of surface oxygen vacancies because the Au deposition was done in vacuum condition. Thus, Au atoms observed here are more likely to attach to the vacancy sites.

Figures 2(a)–2(e) show typical atomic-resolution HAADF STEM plan-view images of Au nanoparticles on a TiO_2 (110) surface, arranged in order of projected particle size. It is seen that the atomic structures of both Au and TiO_2 can be simultaneously resolved. In the case of very small Au islands ($<\sim 2$ nm), as in Figs. 2(a) and 2(b), the strong image intensities corresponding to Au atoms are found on the Ti-O columns and on the O columns along the trough of the Ti-containing columns [along the arrows in the magnified image in Fig. 2(f)]. The strong preference of Au atom attachments on the Ti-O columns is consistent with the Au single atom cases. The present results suggest that Au atoms in the small Au islands also preferentially attach to specific sites on the TiO_2 surface, and therefore form an epitaxial coherent-type heterointerface [19]. These epitaxial Au islands are not only small in size, but are also very thin (a few atomic layers) as estimated from the STEM image intensity profiles. If the Au atoms on the Ti-O columns are in the first Au atomic layer, Au atoms on the trough of Ti-containing columns (on top of O columns) can be considered as second layer atoms, because nearest Au-Au distances would be too close to each other (less than 80% of the stable Au-Au interatomic distance in bulk Au)

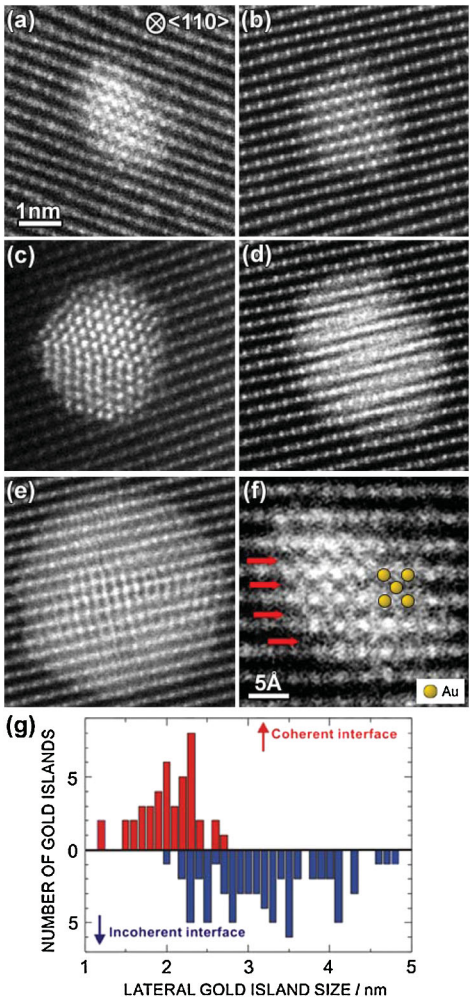

FIG. 2 (color). (a)–(e) HAADF STEM images of Au nanoparticles arranged in order of projected particle size. The lattice coherency between Au nanoparticles and TiO_2 substrate clearly changes according to the Au particle size [(a) and (b) are coherent, but (c)–(e) are incoherent]. (f) Magnified image of the epitaxial Au structure shown in (a). Not only Au sites on top of Ti-O columns, but also Au sites on top of O columns in the troughs of Ti-containing columns (along the arrows) are resolved. (g) A histogram of the formation of coherent or incoherent interfaces as a function of Au nanoparticle lateral size estimated from the HAADF STEM images.

if these Au atoms were on the same first atomic layer. This proposed Au bilayer stacking sequence is similar to the (110) stacking ($\{110\}_{Au} \parallel \{110\}_{TiO2}$, $\langle 100\rangle_{Au} \parallel \langle 110\rangle_{TiO2}$) or (100) stacking ($\{100\}_{Au} \parallel \{110\}_{TiO2}$, $\langle 110\rangle_{Au} \parallel \langle 110\rangle_{TiO2}$) of fcc Au on TiO_2 (110), despite the extremely large lattice mismatch ($>20\%$) in one direction.

On the other hand, if the Au size becomes larger ($> \sim 3$ nm), as in Figs. 2(c)–2(e), various orientation relationships exist between the Au nanoparticles and the TiO_2 substrate. Frequently observed moiré fringes [20] suggest that the lattices are gradually displaced or rotated from each other. These results indicate that the Au/TiO_2 (110) interface is not a coherent interface, but an

incoherent-type heterointerface [19], which is often found in large-mismatched metal-oxide heterointerface systems [21,22]. Figure 2(g) shows a histogram of the formation of coherent or incoherent interfaces as a function of the projected Au nanoparticle size. Although the thickness of the Au nanoparticles along the beam direction is difficult to precisely estimate, our systematic observations strongly suggest that there is a structural transition at the Au/TiO_2 (110) interface for Au particles around 2–3 nm in size.

To verify the structural transition at the Au/TiO_2 interfaces theoretically, first-principles DFT calculations were performed on model $Au(110) \parallel TiO_2(110)$ interfaces, whose interface orientation is based on the one estimated from the STEM images in Fig. 2. The projector augmented wave method, implemented in the VIENNA *ab initio* simulation package, was used [23]. The electron exchange-correlation potential was described by the generalized gradient approximation in the form of Perdew, Burke, and Ernzerhof [24]. Spin polarization was included throughout the calculations. Brillouin-zone sampling using a $1 \times 8 \times 1$ Monkhorst-Pack mesh [25] (four irreducible k points) was performed for the Au/TiO_2 supercells. It was confirmed that these conditions ensured a good total energy convergence of 1 meV/atom for the Au/TiO_2 supercells.

To estimate the effect of Au nanoparticle mass on the interface structure, two interface models with two (thin) and nine (thick) Au atomic layers stacked on the TiO_2 surfaces were simulated [26]. To allow for the large interfacial misfits in the simulation, the TiO_2 (110) and Au (110) surface units were extended by 1×5 and 1×8, respectively, to minimize the total lattice mismatch between the extended TiO_2 and Au slabs in the initial structure. According to our systematic DFT calculations, the stable termination of TiO_2 in the interface formation is strongly dependent on the external atmosphere and the reduced TiO_2 surface termination is more stable than the stoichiometric one in the reducing atmosphere [27]. Because our Au deposition was done in a reducing atmosphere, the reduced TiO_2 (110) termination model for the initial Au/TiO_2 interface models was used. In fact, the reduced interface model can reasonably reproduce the Au island structure observed by STEM. DFT calculations of the same two-layer Au on the stoichiometric TiO_2 (110) surface were also performed, but the results were inconsistent with our experimental observation.

Figures 3(a) and 3(b) show the relaxed structures of the respective interface models. In the case of the two-layer model, Au atoms significantly relax their positions: Au atoms in the first layer move to the on-top sites of the Ti-O columns (O_{br} vacancy sites), whereas Au atoms in between these sites merge into the top surface layer. As a result, the Au structure shows the unique structural feature that the second Au layer is attached on the first Au layer rigidly anchored by the TiO_2 substrate. The Au atomic positions in the epitaxial islands are consistent with our experimental observations, which can also be confirmed from the STEM image simulation shown in the inset.

In the case of the nine-layer model, the relaxed structure shows no obvious lattice coherency at the Au/TiO_2 inter-

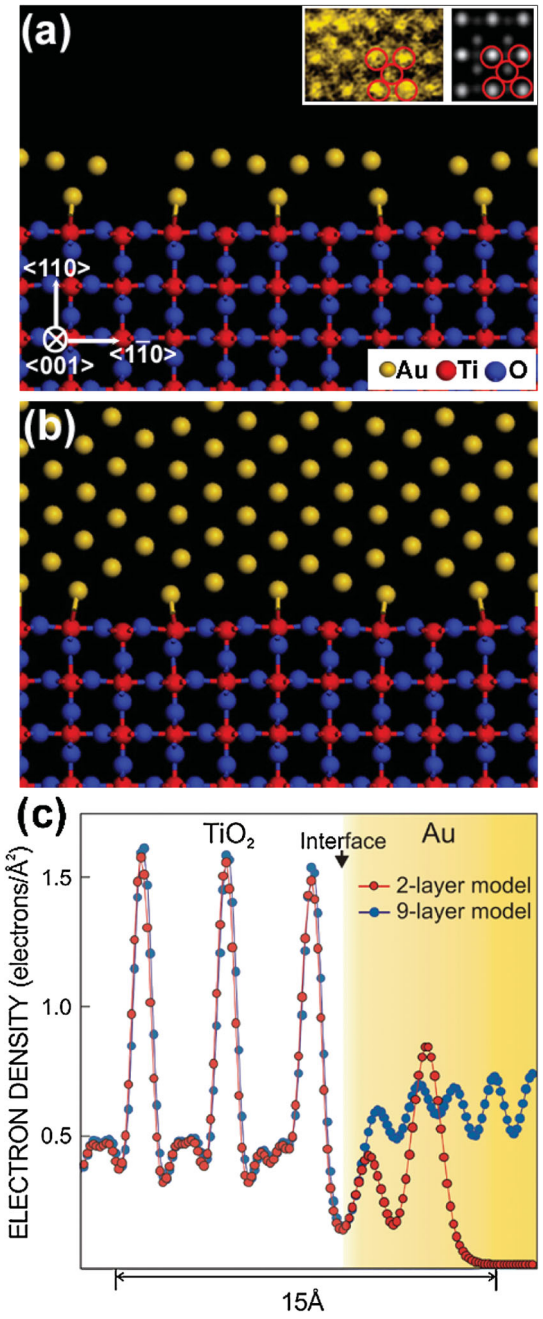

FIG. 3 (color). DFT-relaxed atomic structures of Au/TiO_2 interfaces with (a) two atomic-layer Au and (b) nine atomic-layer Au on the reduced TiO_2 (110) surface. Insets in (a) show the comparison between experimental and simulated HAADF STEM images based on the DFT obtained epitaxial Au structure viewed from ⟨110⟩ plan-view direction. (c) The total electron density profiles projected onto the atomic layers across the Au/TiO_2 interfaces in the two models. According to the Barder charge analysis [28] of our DFT results, the extra negative charge per Au atom in the two-layer model is estimated to be −0.15 electron/atom.

face. The first layer Au atoms are likely to move their position to the stable sites as in the two-layer model, but the thick atomic layers above the first layer prevent any drastic structural relaxation at the interface. Thus the interface keeps incoherentlike structure as in the initial unrelaxed structure. The present results indicate that the interfacial coherency is strongly dependent on the mass of Au nanoparticles, consistent with our experimental observations.

Figure 3(c) shows the total electron density projected onto the atomic layers across the Au/TiO_2 interfaces in the above two models. An anomalous increase in the electron density is found at the top surface Au layer in the two-layer model. This is attributed to the increased atomic density at the top surface layer of the reconstructed Au structure. Moreover, electron transfer from the reduced TiO_2 surface to the Au layers is observed. The reconstructed electronic structure of the two-layer Au is thus completely different from that of bulk Au. In contrast, the electron density change in the Au structure in the nine-layer model is much smaller and limited to within a few atomic layers from the interface. Above those interface layers, the electron density of Au becomes similar to that of the bulk Au. These results suggest that the electronic structure of Au nanoparticles is strongly influenced by the structure of the nanoscale heterointerface.

In summary, the present study demonstrates that the atomic structure of Au nanoparticles is strongly influenced by the supporting TiO_2 surfaces. When the Au nanoparticles are very small and atomically thin, the strong templating behavior of the TiO_2 surface reconstructs both the atomic and the electronic structure of the Au nanoparticles. When the Au nanoparticle size becomes larger and thicker, the interface loses lattice coherency in order to accommodate large lattice mismatch, and the support effect rapidly decays across the interface. Our systematic observations thus clearly show that there is a structural transition at the Au/TiO_2 (110) interface depending on the Au particle size. We believe the strong interaction between nanosized Au and oxide support via unique nanoscale heterointerface structure will be an essential factor in understanding the origin of size-dependent catalytic activity of Au nanoparticles supported on metal oxides.

This work was supported in part by the Grant-in-Aid for Scientific Research on Priority Areas ''Nano Materials Science for Atomic-scale Modification 474'' from the Ministry of Education, Culture, Sports and Technology (MEXT) of Japan. N. S. acknowledges support from PRESTO, Japan Science and Technology Agency, and from New Energy and Industrial Technology Development Organization (NEDO). S. D. F. is supported by the Japan Society for the Promotion of Science (JSPS).

*shibata@sigma.t.u-tokyo.ac.jp

[1] M. Haruta, N. Yamada, T. Kobayashi, and S. Iijima, J. Catal. **115**, 301 (1989).
[2] M. Valden, X. Lai, and D. W. Goodman, Science **281**, 1647 (1998).
[3] T. Hayashi, K. Tanaka, and M. Haruta, J. Catal. **178**, 566 (1998).
[4] F. Boccuzzi *et al.*, J. Catal. **188**, 176 (1999).
[5] M. Haruta, Catal. Today **36**, 153 (1997).
[6] P. D. Nellist and S. J. Pennycook, Science **274**, 413 (1996).
[7] S. N. Rashkeev *et al.*, Phys. Rev. B **76**, 035438 (2007).
[8] S. J. Pennycook and D. E. Jesson, Ultramicroscopy **37**, 14 (1991).
[9] R. Nakamura *et al.*, J. Phys. Chem. B **109**, 1648 (2005).
[10] Y. Lu, B. Jaeckel, and B. A. Parkinson, Langmuir **22**, 4472 (2006).
[11] N. Shibata *et al.*, Science **322**, 570 (2008).
[12] L. J. Allen, S. D. Findlay, M. P. Oxley, and C. J. Rossouw, Ultramicroscopy **96**, 47 (2003).
[13] Y. Wang and G. S. Hwang, Surf. Sci. **542**, 72 (2003).
[14] K. Okazaki *et al.*, Phys. Rev. B **69**, 235404 (2004).
[15] A. Vijay, G. Mills, and H. Metiu, J. Chem. Phys. **118**, 6536 (2003).
[16] E. Wahlström *et al.*, Phys. Rev. Lett. **90**, 026101 (2003).
[17] Z. X. Yang, R. Wu, and D. W. Goodman, Phys. Rev. B **61**, 14 066 (2000).
[18] D. Matthey *et al.*, Science **315**, 1692 (2007).
[19] D. Wolf, in *Materials Interfaces: Atomic-Level Structure and Properties*, edited by D. Wolfand and S. Yip (Chapman and Hall, London, 1992), pp. 1–57.
[20] D. B. Williams and C. B. Carter, *Transmission Electron Microscopy: A Textbook for Materials Science. Imaging III* (Plenum Press, New York, 1996), pp. 441–455.
[21] Y. Ikuhara *et al.*, Philos. Mag. A **70**, 75 (1994).
[22] K. Matsunaga *et al.*, Phys. Rev. B **74**, 125423 (2006).
[23] G. Kresse and D. Joubert, Phys. Rev. B **59**, 1758 (1999).
[24] J. P. Perdew, K. Burke, and M. Ernzerhof, Phys. Rev. Lett. **77**, 3865 (1996).
[25] H. J. Monkhorst and J. D. Pack, Phys. Rev. B **13**, 5188 (1976).
[26] In the two-layer model, one atomic layer of Au was initially relaxed on the TiO_2 surface, and then the next Au (110) layer was stacked and relaxed on the stable one-layer structure. The Au surfaces were separated by a vacuum space about 1 nm thick.
[27] We performed thermodynamic analyses of the TiO_2 (110) surface energy and the Au-TiO_2 interface energy based on the DFT results. Compared to the stoichiometric case, we found that the reduced TiO_2 (110) surface is unstable over a wide range of oxygen chemical potential, whereas the reduced Au/TiO_2(110) interface becomes more stable in relatively low oxygen chemical potential.
[28] G. Henkelman, A. Arnaldsson, and H. Jónsson, Comput. Mater. Sci. **36**, 354 (2006).